International Journal of Electrical, Electronic and Communication Sciences
ISSN: 2517-9438
Vol:13, No:9, 2019

Optimization of Solar Rankine Cycle by Exergy Analysis and Genetic Algorithm

R. Akbari, M. A. Ehyaei, R. Shahi Shavvon

Abstract**—**Nowadays, solar energy is used for energy purposes such as the use of thermal energy for domestic, industrial and power applications, as well as the conversion of the sunlight into electricity by photovoltaic cells. In this study, the thermodynamic simulation of the solar Rankin cycle with phase change material (paraffin) was first studied. Then energy and exergy analyses were performed. For optimization, a single and multi-objective genetic optimization algorithm to maximize thermal and exergy efficiency was used. The parameters discussed in this paper included the effects of input pressure on turbines, input mass flow to turbines, the surface of converters and collector angles on thermal and exergy efficiency. In the organic Rankin cycle, where solar energy is used as input energy, the fluid selection is considered as a necessary factor to achieve reliable and efficient operation. Therefore, silicon oil is selected for a high-temperature cycle and water for a low-temperature cycle as an operating fluid. The results showed that increasing the mass flow to turbines 1 and 2 would increase thermal efficiency, while it reduces and increases the exergy efficiency in turbines 1 and 2, respectively. Increasing the inlet pressure to the turbine 1 decreases the thermal and exergy efficiency, and increasing the inlet pressure to the turbine 2 increases the thermal efficiency and exergy efficiency. Also, increasing the angle of the collector increased thermal efficiency and exergy. The thermal efficiency of the system was 22.3% which improves to 33.2 and 27.2% in single-objective and multi-objective optimization, respectively. Also, the exergy efficiency of the system was 1.33% which has been improved to 1.719 and 1.529% in single-objective and multi-objective optimization, respectively. These results showed that the thermal and exergy efficiency in a single-objective optimization is greater than the multi-objective optimization.

Keywords**—**Exergy analysis, Genetic algorithm, Rankine cycle, Single and Multi-objective function.

I. Introduction

CONSUMPTION of fossil fuels has several disadvantageous such as greenhouse gas emissions, global warming, and environmental degradation besides shortage of fossil fuels have caused a major consideration to use of clean and renewable energies.

Iran with area of 1,648,195 km^2 is a rich country in terms of non-renewable energy resources which has the world's second largest natural gas reserves and the OPEC's second largest supply of oil [1]. With an average annual rainfall of 228 mm, Iran is classified as arid and semi-arid country [2]. Deserts of Iran receive daily solar irradiation of about 5 kWh/m^2, so solar energy appears as the most promising technology to lead the Iran's economic sector towards sustainability [3]. In recent years, the electricity demand is increasing and optimizing sources of energy regarding to condition of environment and general supply of energy is needed. Solar energy has been considered as the most promising option for power generation nowadays and in the future [4]. Solar photovoltaic systems and solar thermal systems are the two methods for capturing the solar energy to generate power [5].

One the most common power generation cycle to produce electricity from solar thermal energy is the Rankine cycle [6]. The main components of a solar thermal Rankine system are the solar collector, the thermal energy storage, a boiler, a turbine, a condenser and a pump. In a solar Rankine cycle, thermal energy from the sun is utilized by means of a solar collector which acts as an evaporator to heat the working fluid of the Rankine cycle either directly or indirectly [7]

Performance improvement of Rankine cycle using Genetic algorithm and exergy analysis have been studied by several researchers. For example, Mishra and Khan discussed Exergy and energy analysis of organic Rankine cycle for reduction of global warming and ozone depletion [8]. Ahmed and Mahanta used genetic algorithm for simultaneously maximizing three objective functions - exergy efficiency, thermal efficiency, and specific network in of an organic Rankine cycle (ORC) integrated with a power generating stationary diesel engine [9]. Ghasemian and Ehyaei studied optimization of organic cycle for eight subcritical coolant fluids using with algorithms NSGA-II, MOPSO, and MOEA [10].

To improve efficiency of solar Rankine cycles different modifications have been performed. These modifications include use two stages of Compound Parabolic Collector collectors [11], use of main collector, and flat plate collector [12], hybrid power systems that is a popular form that integrated solar combined cycle systems (ISCCS) [13].

In this study, solar Rankine cycle is optimized using Genetic Algorithm. Single-objective optimization involves optimizing thermal and exergy efficiency and multi-objective optimization is performed for simultaneously maximizing two objective functions thermal and exergy efficiency and minimizing the total exchanger's level of the system. The performances of each of the optimization are compared. In order to analyze the thermodynamics, some changes were made to the design parameters of the system, and then the impact of these changes on the performance of the cycle and the thermal and exergy efficiency of the system are investigated.

R. Akbari is with Lamerd Branch Islamic Azad University, Fars, Iran (phone: +989129367314; e-mail: r.akbari@iaulamerd.ac.ir).
M. A. Ehyaei is with Pardis Branch Islamic Azad University, Tehran, Iran (phone: +98-9123478028; e-mail: aliehyaei@yahoo.com).
R. Shahi Shavvon is with Yasouj University, Yasuj, Iran (phone: +987431001000; w-mail: r.shahi@yu.ac.ir).

II. Math

A. System Description and Assumption

Fig. 1 illustrates the proposed solar Rankine cycle. The cycle has made of two parts: the first one is constructed from collector and thermal energy storage and the second part is a Rankine cycle. The main energy source of the whole system is evacuated by solar collector.

B. Selection of Operating Fluid

In Rankine cycle where solar energy is used as input energy, fluid selection is considered as a necessary factor in order to achieve maximum efficiency. In addition, the chemical stability, environmental impacts and costs should be considered. Most liquids in the Rankin cycle are poisonous and flammable, which causes the destruction of the ozone layer and global warming. In this thesis, silicon oil was selected as the working fluid for a high temperature cycle and water for a low temperature cycle.

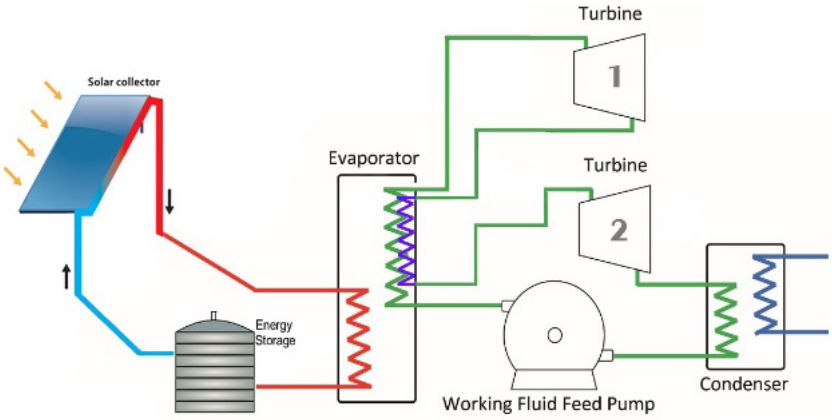

Fig. 1 The proposed solar Rankine cycle

C. Phase Change Material

The phase change materials for thermal storage must have appropriate kinetic, chemical and thermophysical properties. Paraffin RT31 is used as a phase change material from Rubitherm Corporation. The characteristics of the paraffin are presented in Table I.

TABLE I
THE CHARACTERISTICS OF THE PARAFFIN

Latent heat	150 kJ/kg
Melting point	304 K
Density in solid phase	870 kg/m^3
Density in liquid phase	760 kg/m^3
Specific heat capacity	1800-2400 J/kg.K
Thermal conductivity	0.2 W/m.K
Flash point	437 K

In the analysis of the solar Rankine cycle, the following assumptions are considered:

1. All processes in the thermodynamic cycle are fixed.
2. The working fluid of the thermodynamic cycle was assumed to be water. But, with respect to the temperature range, the fluid can be changed according to the relevant thermodynamic cycle (Rankin Steam cycle or Rankine organic cycle).
3. The temperature direct transfer of the system components to the environment is neglected.
4. The kinetic energy and potential changes in various components are neglected.
5. Pump and turbine are adiabatic.
6. Pumps and turbines have certain isentropic yields.
7. The outlet working fluid from the condenser and inlet to the pump is a saturated fluid.

D. Mathematical Modelling

In this study, thermodynamic and exergetic modelling of solar Rankine cycle in Tehran power plant, and its single and multi-objective optimization were performed in MATLAB software.

The rate of absorbed energy by solar flat plate collector is obtained from the following equations [14].

$$S = I_b R_b (\tau\alpha)_b + I_d (\tau\alpha)_d \cdot \frac{(1+\cos\beta)}{2} + (I_b + I_d)(\tau\alpha)_g \cdot \rho_g \frac{(1+\cos\beta)}{2} \quad (1)$$

In (1), the indices b, d, g are due to direct radiation, scattered radiation from the sky and scattered radiation due to the reflection of the ground surface. *I* is the intensity of radiation on the horizontal surface by considering the effect of the environment dust which is calculated based on reference [15].

The constant values that are determined by experimental results are multiplied by the amount of radiation intensity, and ultimately the amount of these quantities are determined. Moreover, $\tau\alpha$ is transmission absorption coefficient, β is the

solar collector slope and the ρ_g is the reflection coefficient of the Earth's surface and it is equal to 0.93. R_b is a dimensionless parameter and represents the scattered radiation of the sky and it is expressed as [14], [15]:

$$R_b = \frac{\cos\theta}{\cos\beta} \tag{2}$$

In this case, ɵ is the angle of sunlight with the collector surface. The scattered radiation is calculated as [14]:

$$\frac{I_d}{I_t} = \begin{cases} 1-0.09k_T & k_T < 0.22 \\ 0.9511-0.1604k_T+4.388k_T^2 & 0.22 < k_T < 0.8 \\ \quad -16.638k_T^2+12.336k_T^4 & \\ 0.165 & k_T > 0.8 \end{cases} \tag{3}$$

In this case, k_T is dimensionless and is the average monthly clearance coefficient.

The general heat loss of collector is obtained from [14]:

$$\dot{Q}_{Loss} = U_L A\left(T_p - T_a\right) \tag{4}$$

In the equation, U_L is the total heat transfer coefficient, A is the collector area, and Ta is the ambient temperature. To obtain the total heat transfer coefficient, the following relationship exists [14]:

$$U_L = U_t + U_b + U_e \tag{5}$$

U_e, U_b are the total heat transfer from the sides and the bottom, and U_t is the overall heat transfer coefficient from above of collector, which is in terms of. U_t is calculated from [14].

$$U_t = \frac{C}{T_p}\left(\frac{T_p - T_a}{1+f}\right)^{0.33} + \frac{1}{h_w} + \frac{\sigma\left(T_p^2+T_a^2\right)\left(T_p+T_a\right)}{\frac{1}{\varepsilon_p}+0.05\left(1+\varepsilon_p\right)+\frac{1+f}{\varepsilon_c}-1}\frac{x-\mu}{\sigma} \tag{6}$$

In the equation, $h_w = 2.6+3V_{wind}$ is the forced heat transfer coefficient between the glass cover exposed to ambient air, which is determined in terms of wind speed (V_{wind}) in terms of. Also, ε_p, ε_C is the diffusion coefficient for absorption plate and the glass cover for infrared radiation, respectively. Also, σ is Stephen Boltzmann's constant. In addition, parameters C and f are calculated from [14].

$$C = 365.9\left(1-0.00883\beta+0.0001298\beta\right) \tag{7}$$

$$f = 1.091\left(1-0.04h_w+0.0005h_w\right) \tag{8}$$

β is the solar collector slope. The amounts of U_e, U_b are calculated as [14]:

$$U_b = \frac{k_b}{L_b} \tag{9}$$

$$U_e = \frac{k_e}{L_e} \tag{10}$$

In the equations Lb, kb, is the width and thermal conductivity coefficient of the insulation plate which located below the absorbent plate. Also, Le and ke are the thickness and thermal conductivity coefficient insulation plate which is located on the sides of the absorbent plate. The useful heat gain rate and plate temperature are calculated by [14]:

$$\dot{Q}_{SC} = AF_R\left(I_t(\tau\alpha) - U_L\left(T_i - T_a\right)\right) \tag{11}$$

$$T_p = T_i + \frac{\dot{Q}_{SC}}{AF_R U_L}\left(1-F_R\right) \tag{12}$$

I_t, τα, T_i and A are direct radiation flux on the slope plate, transmission absorption coefficient, temperature of the fluid to collector and collector area, respectively. Also, F_R is the harvesting factor of the collector and it is calculated from [14]:

$$F_R = \frac{\dot{m}Cp}{AU_L}\left[1-e^{-\left(\frac{U_L F' A}{\dot{m}Cp}\right)}\right] \tag{13}$$

In that equation, $\dot{m}$ and Cp are the massflow rate of water entering the collector and specific heat at a constant pressure of the water, respectively. Also, F' is an efficiency coefficient of the collector, which calculated by [14]:

$$F' = \frac{\frac{1}{U_L}}{W\left[\frac{1}{U_L\left(D_o+W-D_o\right)F}+\frac{1}{C_b}+\frac{1}{\pi D_i h_{fi}}\right]} \tag{14}$$

In the relation W, Di and Do are the distance between the pipes in the collector, the inner diameter and the outer diameter of the fluid tube. Also, Cb= 0.027 and hfi are the conduction coefficient of the substances which connecting tube to absorber plate and heat transfer coefficient of fluid, respectively. The last parameter is calculated according to the Chininskian relation [16].

Also, the heat transfer rate of the solar collector can be obtained by [16]:

$$\dot{Q} = U \cdot A \cdot LMTD \tag{15}$$

where, U, A, and $LMTD$ are the heat transfer coefficient, the area of the heat exchanger and the logarithmic mean temperature difference, respectively [16].

The logarithmic mean temperature difference is defined:

$$LMTD = \frac{\Delta T_A - \Delta T_B}{\ln(\frac{\Delta T_A}{\Delta T_B})} \quad (16)$$

In this model, the reservoir tank is a storage tank with silicon oil. The returned fluid from the collector and the fluid entering from the hot water is completely mixed. In addition, the heat loss of the storage tank is calculated based on the defined efficiency (η_{TST}) in accordance with reference [17]. Therefore, by uniformly assuming the fluid temperature in the tank and neglecting the potential and kinetic energy, the energy conservation to the storage tank is calculated as [17]:

$$mC_p \frac{dT}{dt} = \eta_{TST}\left(\dot{Q}_{net}\right) \quad (17)$$

where T is the mean temperature of the storage tank, m is the stored mass inside the tank, t represents the time and $\dot{Q}_{net}$ is the net heat transfer of the tank.

Exergy can be separated into four parts. Physical exergy and chemical exergy are the two important types of the exergy. In this study, two components of kinetic exergy and potential exergy are neglected. By application of the first and second law of thermodynamics, the following exergy equilibrium is found [18]:

$$\dot{E}x_Q + \sum_i \dot{m}_i ex_i = \sum_e \dot{m}_e ex_e + \dot{E}x_W + \dot{E}x_D \quad (18)$$

where, $\dot{E}x_Q$, $\dot{m}_i$ and ex_i are the heat transfer exergy flows, the inlet mass flow rate and specific exergy for i stream. Also, $\dot{m}_e$, ex_e, $\dot{E}x_W$ and $\dot{E}x_D$ are the outlet mass flow rate and specific exergy, exergy flows of the work and rate of exergy destruction, respectively.

The physical exergy of a stream i is defined as follows [18]:

$$ex = (h_i - h_0) - T_0(s_i - s_0) \quad (19)$$

In the equation ex, h_i, h_0, T_0, s_i, and s_0 are the specific exergy, the inlet enthalpy of the enthalpy of fluid at reference conditions, the ambient temperature, the entropy of stream i and the entropy at reference condition, respectively.

The first and second efficiency based on thermodynamics laws is calculated by the subsequent relationships:

$$\eta_I = \frac{\dot{W}_T - \dot{W}_P}{\dot{Q}_E} \quad (20)$$

$$\eta_{II} = \frac{\dot{W}_T - \dot{W}_P}{I_g \times A\left[1 + \frac{1}{3}\left(\frac{T_a}{T_{sun}}\right)^4 - \frac{4}{3}\left(\frac{T_a}{T_{sun}}\right)\right]} \quad (21)$$

III. Results

A. Thermodynamic Study of Solar Rankine Cycle

The thermodynamic performance of the system which is conducted by the thermodynamic simulation of the system is presented in Table II.

TABLE II
THERMODYNAMIC PERFORMANCE OF THE SYSTEM

Total collectors level (m^2)	1750
Inlet energy to the system (kW)	1623
Thermal efficiency (%)	24/18
Exergy efficiency (%)	1/32
Total surface of the exchanger (m^2)	870

In order to analyze the thermodynamics, some changes were made to the design parameters of the system, and then the impact of these changes on the performance of the cycle and thermal and exergy efficiency of the system was investigated.

B. Effect of Inlet Mass Flow Rate of Turbine 1 on Thermal and Exergy Efficiency

As the mass flow rate increases from turbine 1 to turbine 2, the inlet energy is increased as shown in Fig. 1. The outlet energy of the system also increases from 352.6 kW to 359.8 kW. The thermal efficiency of the system has also increased slightly, as shown in Fig. 1.

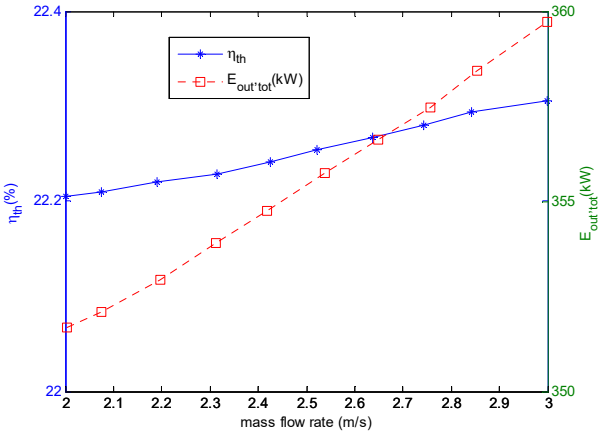

Fig. 1 Changes of thermal efficiency vs. inlet mass flow rate of turbine 1

By increasing the inlet mass flow rate to the turbine 1, the total exergy decreases from 19.95 kW to 17.97 kW. Due to the persistence of solar exergy, the total fuel exergy of the whole system remains constant and its value is 1515 kW. The changes in the exergy efficiency and total exergy relative to the inlet mass flow rate to the turbine 1 are shown in Fig. 2, in which the amount of exergy efficiency is reduced by 14.9%.

C. The Effect of the Inlet Mass Flow Rate to the Turbine 1 on the Total Level of Exchangers

By increasing the inlet mass flow rate to the turbine 1, the total level of the heat exchangers and the level of the

evaporator and condenser increased. The effects of the inlet mass flow rate to the turbine 1 on the total surface of the heat exchangers are shown in Fig. 3.

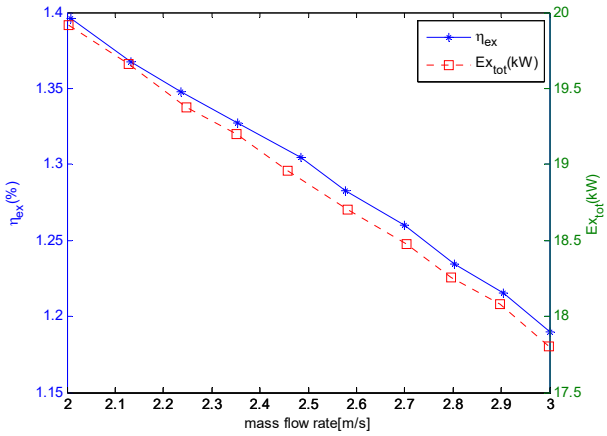

Fig. 2 Changes of exergy efficiency vs. inlet mass flow rate of turbine 1

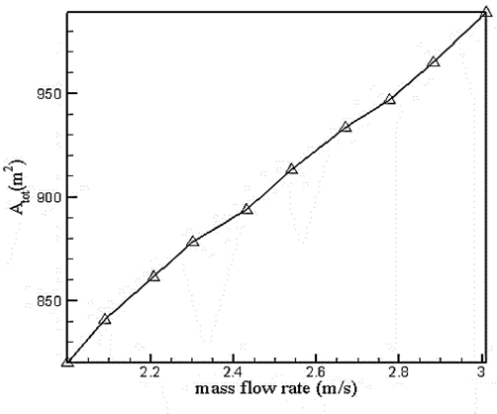

Fig. 3 Changes of the total level of exchangers vs. inlet mass flow rate of turbine 1

D.The Effect of the Inlet Mass Flow Rate to the Turbine 2 on Thermal and Exergy Efficiency

By increasing the inlet mass flow of turbine 2 from 1.5 kg to 1.7 kg, the inlet energies to the system increase. The outlet energy of the system increases from 307.6 kW to 361.7 kW too. The net inlet power of the system increases as well. The amount of inlet energy of the system is the sun, which will remain steady due to the constant amount of sunlight and collector surface. The thermal efficiency of the system also increased from 19.5% to 21.8% (Fig. 4). The results showed that exergy efficiency and total exergy of the system increased (Fig. 5).

E. Effect of Input Pressure to Turbine 1 on Thermal and Exergy Efficiency

As shown in Fig. 6, the outlet energy changes slightly with increasing pressure. The results show that thermal efficiency decreases by 0.12 (Fig. 6). As the inlet pressure to turbine 1 increases, the total exergy decreases by 0.98% (Fig. 7).

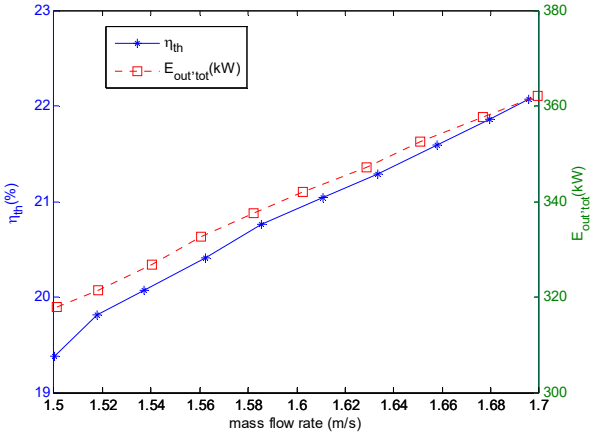

Fig. 4 Changes of thermal efficiency vs. inlet mass flow rate of turbine 2

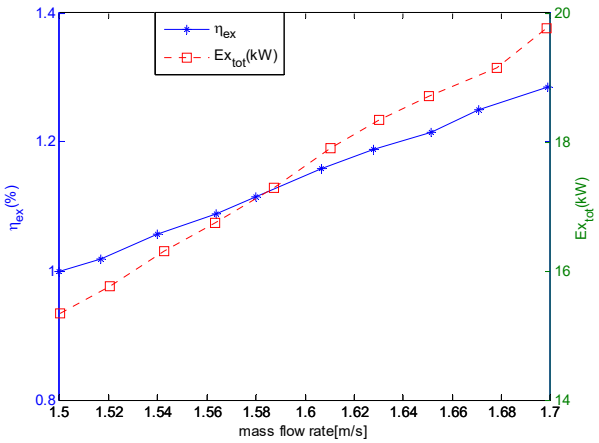

Fig. 5 Changes of exergy efficiency vs. inlet mass flow rate of turbine 2

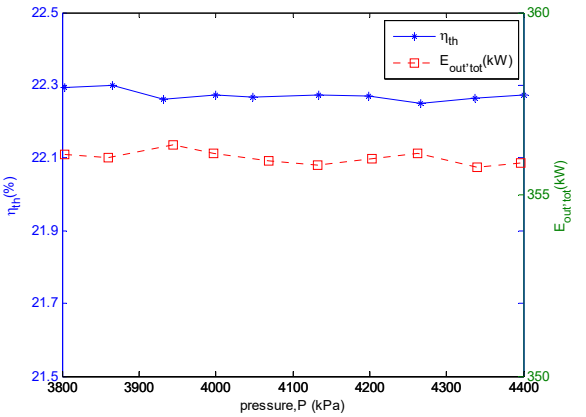

Fig. 6 Changes of thermal efficiency vs. input pressure to turbine 1

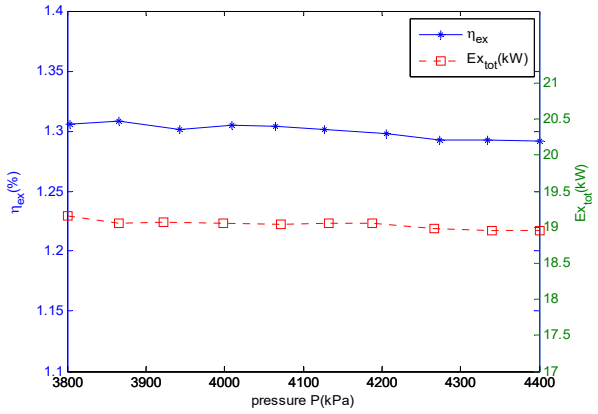

Fig. 7 Changes of exergy efficiency vs. input pressure to turbine 1

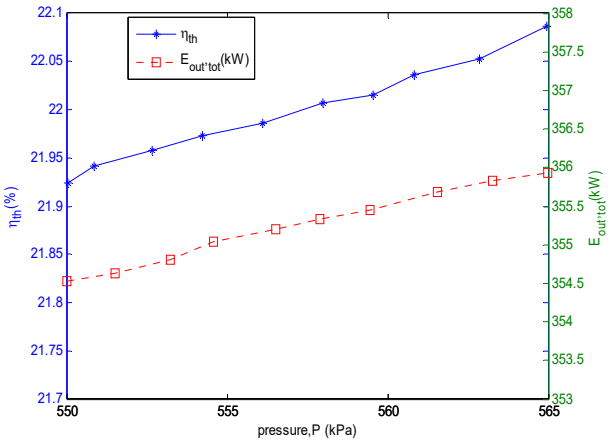

Fig. 8 Changes of thermal efficiency vs. input pressure to turbine 2

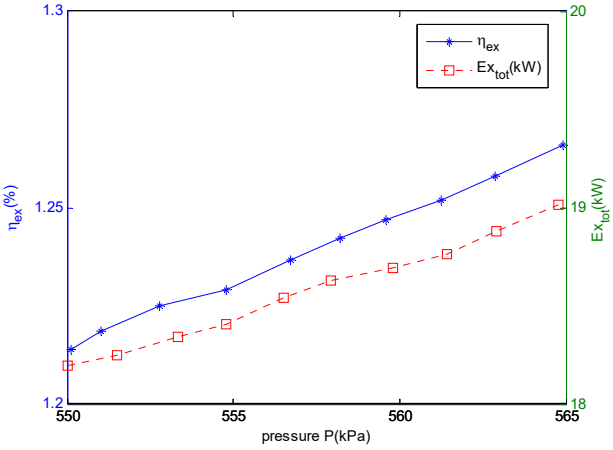

Fig. 9 Changes of exergy efficiency vs. input pressure to turbine 2

F. Effect of Input Pressure to Turbine 2 on Thermal and Exergy Efficiency

Increasing the inlet pressure to the turbine 2 will increase the thermal efficiency and outlet energy (Fig. 8). The effective parameters in the total exergy are: the total evaporator's exergy, the condenser, and the amount of outlet energy from the system. The fuel exergy is related to solar energy, which remains constant due to the persistence of the exergy of the sun. The results show that with increasing pressure inlet to turbine 2, the amount of total exergy and exergy efficiency will increase (Fig. 9).

G. Impact of Collector Tilt Angle with Horizon on Thermal and Exergy Efficiency

As seen in Fig. 10, the total amount of inlet energy of the system decreases from 1648 to 1615 kW by increasing the angle and the efficiency increases slightly.

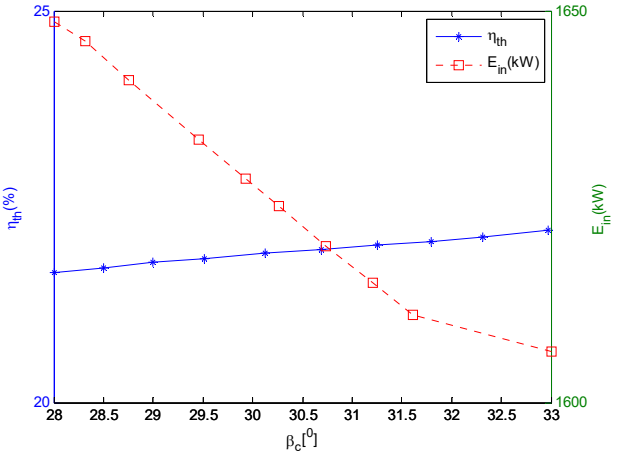

Fig. 10 Changes of thermal efficiency vs. collector tilt angle with horizon

The parameters affecting the total exergy include the condenser, evaporator and the net outlet power of the system. Fig. 11 shows the effect of the collector tilt angle with the horizon on the exergy. According to the diagram, the exergy efficiency and the total exergy will be increased and decreased, respectively.

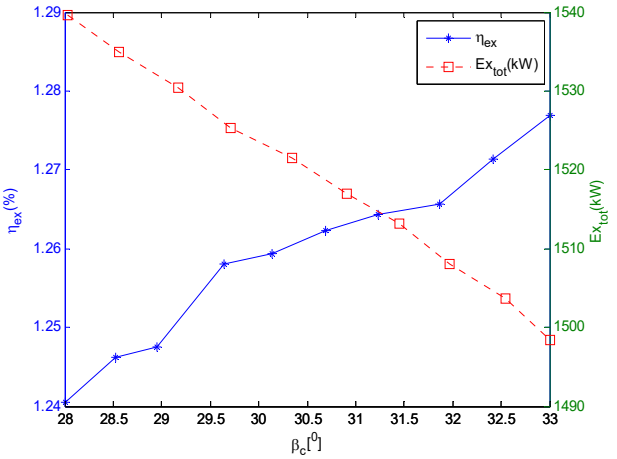

Fig. 11 Changes of exergy efficiency vs. collector tilt angle with horizon

H.Solar Rankine Cycle Optimization

Solar Rankine cycle is optimized by single and multi-objective optimization using Genetic Algorithm. Single-objective optimization involves optimizing thermal and exergy efficiency and multi-objective optimization is performed for simultaneously maximizing two objective functions thermal and exergy efficiency and minimizing the total exchanger's level of the system. Optimization goals include maximizing thermal and exergy efficiency and minimizing the total exchanger's level of the system. The parameters of the genetic algorithm for optimization are presented in Table III.

TABLE III
PARAMETERS OF THE GENETIC ALGORITHM

Parameters	Amount
Number of people per generation	50
Maximum mutation rate	0/2625
Number of generations	50
Initial mutation rate	0/005
Minimum mutation rate	0/0005
cross probability	0/85

1. Single-Objective Optimization

The maximum thermal and exergy efficiency of the system is expressed as follows:

$$\eta_{th} = \frac{\int (\dot{W}_{net} + \dot{Q}_{Eva} + \dot{Q}_{Con2}) d\tau}{\int (A_C G_t) d\tau} \quad (22)$$

$$\eta_{ex} = \frac{\int (\dot{W}_{net} + \dot{E}x_{P,Eva} + \dot{E}x_{P,con2}) d\tau}{\int (\dot{E}x_{Ph,Sun}) d\tau} \quad (23)$$

2. Multi-Objective Optimization

In this section, three parameters of thermal and exergy efficiency and exchanger's level were optimized simultaneously. The LINMAP method is used, which is given by:

$$F_{ij}^{n} = \frac{F_{ij}}{\sqrt[2]{\sum_{i=1}^{m} (F_{ij})^2}} \quad (24)$$

in which F is target function, m is the number of different answers has been obtained and n is the number of target functions. Indices i and j represent the optimization results and target functions, respectively. The shortest distance of the point on the graph from the ideal point is expressed using:

$$d_i = \sqrt{\sum_{j=1}^{n} (F_{ij}^{n} - F_{ideal,j}^{n})^2} \quad (25)$$

Fig. 12 illustrates the multi-objective optimization, including the total surface of the exchangers relative to energy and exergy efficiency. Single-objective and multi-objective optimization results are presented in Table IV.

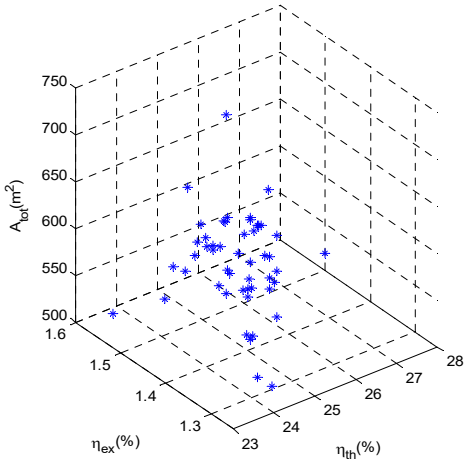

Fig. 12 The multi-objective optimization's result

TABLE IV
SINGLE-OBJECTIVE AND MULTI-OBJECTIVE OPTIMIZATION

		η_{th}[%]	η_{ex}[%]	A_{tot}[%]
Single-objective optimization	Minimum total level of exchangers (m^2)	22/3	1/31	878/7
	Maximum exergy efficiency	33/2	1/538	874/8
	Maximum thermal efficiency	30/17	1/719	725/9
Without optimization		23/83	1/439	525
Multi-objective optimization		27/27	1/529	658/5

The design parameters in the system are: NPV, number of solar panels. Equation (25) shows the range of variations of these parameters:

$$\begin{aligned} N_{PV,\min} \le N_{PV} \le N_{PV,\max} \\ N_{WT,\min} \le N_{WT} \le N_{WT,\max} \\ N_{B,\min} \le N_{B} \le N_{B,\max} \end{aligned} \quad (26)$$

The objective functions and limits can be expressed as:

$$\min \quad IC = \frac{\sqrt{\frac{1}{T_L}.\sum_{t=0}^{T_L}(P_{L,t} - S_t)^2}}{\sqrt{\frac{1}{T_L}.\sum_{t=0}^{T_L}(P_{L,t})^2} + \sqrt{\frac{1}{T_L}.\sum_{t=0}^{T_L}(S_t)^2}} \quad (27)$$

$$\min \quad TNPC(N_{PV}, N_{WT}, P_{DG,n}, N_B) = NPC_{PV} + NPC_{WT} + NPC_{inv} + NPC_{DG} + NPC_B$$

IV. CONCLUSION

The following results can be considered:

1. The highest thermal efficiency without optimization is 22.3%.
2. The highest exergy efficiency without optimization is 1.31.
3. Increasing the inlet mass flow rate to the turbine 1 from 2

to 3 kg/s increased the thermal efficiency by 2.04 and decreased the exergy efficiency by 9.92%.

4. Increasing the inlet mass flow rate to the turbine 2 from 1.5 to 1.7 kg/s increased the thermal and exergy efficiency by 17.58 and 27.7, respectively.
5. Increasing the input pressure to the turbine 1 from 1 to 600 kPa results in a reduction in thermal and exergy efficiency of 0/12% and of 0/98%, respectively.
6. Increasing the input pressure to turbine 2 at 15 kPa increased thermal and exergy efficiency by 0.34% and 4.1%, respectively.
7. Increasing the collector angle from 28 to 32 degrees from the horizon increased the thermal and exergy efficiency by 1.74% and 2.97, respectively.
8. The thermal efficiency of the system is 2/23, which improves the maximum thermal efficiency up to 2/33 in single-objective optimization, which is approximately 27.27% in multi-objective optimization.
9. The exergy efficiency of the system is 1.31% that has been improved up to 1.719% and 529.1% in single-objective and multi-objective optimization, respectively.
10. Total level of exchangers was equal to 878.7 square meters. The level of exchangers decreased to 525 and 658.5 square meters in the single-objective and multi-objective optimization, respectively.

ACKNOWLEDGMENT

We thank our colleagues from the Islamic Azad University, Lamerd Branch who provided insight and expertise that greatly assisted the research.

REFERENCES

[1] S. E. Hosseini, A. M. Andwari, M. A. Wahid, G. Bagheri, S. Ehsan, A. Mahmoudzadeh, and M. Abdul, "A review on green energy potentials in Iran," *Renew. Sustain. Energy Rev*., vol. 27, pp. 533–545, Nov. 2013.

[2] M. Vafaeipour, S. Hashemkhani Zolfani, M. H. Morshed Varzandeh, A. Derakhti, and M. Keshavarz Eshkalag, "Assessment of regions priority for implementation of solar projects in Iran: New application of a hybrid multi-criteria decision making approach," *Energy Convers. Manag.*, vol. 86, pp. 653–663, Oct. 2014.

[3] R. Hosseini, M. Soltani, and G. Valizadeh, "Technical and economic assessment of the integrated solar combined cycle power plants in Iran," *Renew. Energy*, vol. 30, no. 10, pp. 1541–1555, Aug. 2005.

[4] G. Franchini, A. Perdichizzi, S. Ravelli and G. Barigozzi, "A comparative study between parabolic trough and solar tower technologies in Solar Rankine Cycle and Integrated Solar Combined Cycle plants", *Sol Energy,* vol. 98, pp. 302–14, Dec. 2013.

[5] B. Twomey, P. A. Jacobs and H. Gurgenci, "Dynamic performance estimation of small-scale solar cogeneration with an organic Rankine cycle using a scroll expander", *Appl Therm Eng*, vol. 51, pp. 1307–16, Mar. 2013.

[6] C. Tzivanidis, E. Bellos and K. A. Antonopoulos, "Energetic and financial investigation of a stand-alone solar-thermal Organic Rankine Cycle power plant", *Energy Convers Manag,* vol. 126, pp. 421-33, Oct. 2016.

[7] O. Aboelwafaa, K. F. Seif-Eddeen, S. Ahmed and M. I. Ibrahim, "A review on solar Rankine cycles: Working fluids, applications, and cycle Modifications", *Renew. Sustain. Energy Rev*, vol. 82, pp. 868–885, Feb. 2018.

[8] S. H. R. Mishra and Y. Khan, "Exergy and energy analysis of modified organic Rankine cycle for reduction of global warming and ozone depletion", *IJREI*, vol. 1, no. 3, pp. 1-12, Jan. 2017.

[9] Z. Ahmed, K. D. Mahanta, "Optimization of an organic Rankine cycle in energy recovery from exhaust gases of a diesel engine", *IJMET,* vol. 5, no. 12, pp. 97-109, Dec. 2014.

[10] E. Ghasemian and M. A. Ehyaei, "Evaluation and optimization of organic Rankine cycle (ORC) with algorithms NSGA-II, MOPSO, and MOEA for eight coolant fluids", *Int J Energy Environ Eng*, vol. 9, pp. 39-57, Oct. 2017.

[11] L. Jing, P. Gang and J. Jie, "Optimization of low temperature solar thermal electric generation with Organic Rankine Cycle in different areas", *Appl. Energy,* vol. 87, pp. 3355-65, Nov. 2010.

[12] P. Gang, L. Jing and J. Jie, "Design and analysis of a novel low-temperature solar thermal electric system with two-stage collectors and heat storage units", *Renew Energy,* vol. 36, pp. 2324–33, Sep. 2011.

[13] W. J. Yang, C. H. Kuo and O. Aydin, "A hybrid power generation system: solar-driven Rankine engine-hydrogen storage", *Int J Energy Res,* vol. 25, pp. 1107–25, Jun. 2001.

[14] S. A. Kalogirou, "Solar thermal collectors and applications", *Prog. Energy Combust. Sci.,* Vol. 30, no. 3, Apr. 2004.

[15] A. Mokhtari, A. Koppel, G. Scutari, and A. Ribeiro, "Large-scale nonconvexstochastic optimization by doubly stochastic successive convex approximation", in *Acoustics, Speech and Signal Processing* (ICASSP), 2017 IEEE *International Conference on*, pp. 4701–4705.

[16] T. L. Bergman, A. S. Lavine, F. P. Incropera, D. P. Dewitt, D.P., 2011. *Fundamentals of Heat and Mass Transfer*, sixth ed. John Wiley Publications, New Jersey, 2011.

[17] H. Hajabdollahi, "Evaluation of cooling and thermal energy storage tanks in optimization of multi-generation system", *J. Energy Storage,* Vol. 4, pp. 1-13, Dec. 2015.

[18] Y. A. Cengel, M. A. Boles, "*thermodynamics: an engineering approach*", 4th ed. New York, NY: McGraw-Hill, 2002.